Available online at www.sciencedirect.com
SCIENCE DIRECT®
Journal of Molecular Catalysis A: Chemical 210 (2004) 9–16
JOURNAL OF MOLECULAR CATALYSIS A: CHEMICAL
www.elsevier.com/locate/molcata

Metallomicellar catalysis: effects of bridge-connecting ligands on the hydrolysis of PNPP catalyzed by Cu(II) complexes of ethoxyl-diamine ligands in micellar solution

Jiang Fubin [a,b], Jiang Bingying [a], Chen Yong [c], Yu Xiaoqi [a,1], Zeng Xiancheng [a,*]

[a] *Sichuan Key Laboratory of Green Chemistry and Technology, Faculty of Chemistry, Sichuan University, Chengdu 610064, PR China*
[b] *College of Chemistry and Chemical Engineering, Guangxi University, Nanning 530004, PR China*
[c] *Department of Applied Oil Engineering, Logistical Engineering University, Chongqing 400016, PR China*

Received 20 March 2003; received in revised form 12 May 2003; accepted 17 July 2003

Abstract

The syntheses of three ligands are reported: *N*,*N*,*N*′,*N*′-tetra(2-hydroxyethyl)-1,3-propylene-diamine (**1**), *N*,*N*,*N*′,*N*′-tetra(2-hydroxyethyl)-1,10-decadiamine (**2**), *N*,*N*,*N*′,*N*′-tetra(2-hydroxyethyl)-1,4-xylyldiamine (**3**). The catalytic hydrolysis of *p*-nitrophenyl picolinate (PNPP) by the bivalent metal ion Cu(II) complexes of these ligands was studied kinetically in a buffered CTAB or Brij35 micellar solutions at 25 °C and different pH values. The results indicate that 1:2 and 2:1 complexes of these ligands and metal ion are the active species for the catalytic hydrolysis of PNPP in CATB and Brij35 micellar solutions. The ternary complex kinetic model for metallomicellar catalysis was employed to obtain the relative kinetic and thermodynamic parameters. The effects of the structure of the ligands and the microenvironment of reaction on the hydrolytic reaction of PNPP have been discussed in detail.

Keywords: Metallomicellar catalysis; Hydrolysis of PNPP; Metal complex; Kinetics; Bridge-connecting ligand; Microenvironment

1. Introduction

In hydrolytic metalloenzymatic models, many ligands have one or two hydroxyl groups. When they form complex with transition metal ion, one obvious feature is that the hydroxyl group of the ligand or the chelating water molecule acts as a strong nucleophilic group activated by transition metal ion [1–5]; in addition, the location of the transition metal ions in active center plays a very important role in activating substrate and stabilizing the negative charge, especially under the near neutral conditions producing nucleophilic group OH^-. In nature, the metal ion of many hydrolytic metalloenzymes such as carboxypeptidase A, carbonic anhydrasae [6], alkaline phosphatasae [7], is Zn(II). At present, a large number of recent studies on mimicking hydrolytic metalloenzymes have used metal ions Co(III) [8,9], Cu(II) [10,11], Ni(II) [12,13], Ln(III) [14], etc. as the active center of the system, and complexes containing Cu(II) as the metalloenzymatic model are especially successful.

The micellar medium promotes the electrophilicity of metal ions toward micellar-bound substrates in the positively charged Stern layer and the metallomicellar function mimics the structure of the metalloenzymatic active center and the hydrophobic microenvironment [15]. In previous studies on the catalytic hydrolysis of carboxyl acid esters, we investigated hydrolysis of PNPP [16–20] catalyzed by many kinds of metallomicelles composed of various bivalent transition metal complexes in different micellar solutions quantitatively. The effect of the structure of bridged ligands and microenvironment formed from different kinds of surfactants on the catalytic hydrolysis of carboxylic acid esters is seldom reported. Therefore, three kinds of ethoxy-diamine ligands containing hydroxyl group have been synthesized, and in order to further understand the effects of different microenvironments formed from different kinds of surfactants, we studied the hydrolysis of PNPP in the micellar solutions of CTAB or Brij35 in the presence of complexes formed by three ligands and metal ion (Cu^{2+}). A ternary complex kinetic model for metallomicellar catalysis has been de-

* Corresponding author.
E-mail address: zengxc@pridns.scu.edu.cn (Z. Xiancheng).
[1] Co-corresponding author.

1381-1169/$ – see front matter © 2003 Elsevier B.V. All rights reserved.
doi:10.1016/j.molcata.2003.07.019

rived in this paper. The results indicated that the catalytic activity of these complexes formed from different ligands is related to the difference in the bridged ligands and their microenvironments, which has been dissected in detail in this paper.

2. Experimental

2.1. Spectroscopic measurements

^{1}H spectra were obtained on a Brucker DPX-300FX NMR Spectrometer. Mass spectrometry was performed using a Finnigan MAT 45001 mass spectrometer. Infrared spectra were performed by a PE983IFS FIOIP spectrometer. Elemental analyses were performed with a Carlo Erba 1106 instrument. Kinetic studies were carried out by monitoring UV/Vis spectra with a GBC 916 UV/Vis spectrophotometer equipped with a thermostatic cell holder.

2.2. Materials

$Cu(NO_3)_2{\cdot}6H_2O$, CTAB, Brij35, nitric acid, acetonitrile and tri(hydroxymethyl)aminomethane were analytical-grade commercial products. CTAB was recrystallized before use. *p*-Nitrophenyl picolinate (PNPP) was supplied by Organic Chemical Laboratory of Sichuan University [21]. PNPP stock solution for kinetics was prepared in acetonitrile. To avoid the influence of chemical components of different buffers, Tris–TrisH$^+$ buffer was used in all case and its pH was adjusted by adding analytically pure nitric acid in all runs.

2.3. Synthesis and properties of ligands

N,N,N′,N′-tetra(2-hydroxyethyl)-1,3-propylene-diamine (**1**). To a solution of diethanolamine (5.26 g, 0.05 mol) and dried K_2CO_3 (14 g, 0.1 mol) in freshly distilled CH_3CN (80 ml) 1,3-dibromopropane (2.53 ml, 0.024 mol) was added. After the addition was complete, the solution was further stirred (2 h) at room temperature, and then heated under reflux about 72 h. The slurry was subsequently filtered off, and the acetonitrile was evaporated under reduced pressure to give the crude product as oil, which was purified by column chromatography (SiO_2, $CHCl_3/CH_3OH/NH_3{\cdot}H_2O$ 3:1:0.2). The yield of compound **1** is 53% as colorless oil. ^{1}H NMR (300 MHz, $CDCl_3$): δ 1.70 (m, 2H), 2.55 (m, 4H), 2.60 (m, 8H), 3.65 (t, 8H). IR (KBr pellet): 3335, 2950, 1654, 1458, 1036. Anal. Calcd. for $C_{11}H_{26}N_2O_4$: C, 52.78, H, 10.47, N, 11.19; found: C, 52.51, H, 10.40, N, 11.09. MS: 251 ($M^+ + 1$).

N,N,N′,N′-tetra(2-hydroxyethyl)-1,10-decadiamine (**2**). This compound was synthesized by the same procedure for compound **1**. 1,10-Dibromodecane took the place of 1,3-dibromopropane in use. The yield of compound **2** is 40% as yellow solid, m.p. 25–28 °C. ^{1}H NMR (300 MHz, $CDCl_3$): δ 1.28 (m, 16H), 1.45 (t, 4H), 2.50 (t, 4H), 2.64 (t, 8H), 3.61 (t, 8H). IR (KBr pellet): 3322, 2914, 1470, 1088, 724. Anal. Calcd. for $C_{18}H_{40}N_2O_4$: C, 62.03, H, 11.57, N, 8.04; found: C, 61.98, H, 11.50, N, 8.01. MS: 349 ($M^+ + 1$).

N,N,N′,N′-tetra(2-hydroxyethyl)-1,4-xylyldiamine (**3**). This compound was synthesized by following the same procedure for compound **1**. α,α′-Dibromo-*p*-xylene took the place of 1,3-dibromopropane in use. The yield of compound **3** is 43% as yellow solid, m.p. 20–25 °C. ^{1}H NMR (300 MHz, $CDCl_3$): δ 2.66 (t, 8H), 3.26 (broad, 4H), 3.56 (t, 8H), 3.64 (s, 4H), 7.30 (s, 4H). IR (KBr pellet): 3332, 2872, 1662, 1448, 1038, 824. Anal. Calcd. for $C_{16}H_{28}N_2O_4$: C, 61.51, H, 9.03, N, 8.97; found: C, 61.33, H, 9.02, N, 8.87. MS: 313 ($M^+ + 1$).

2.4. Kinetics

Kinetic measurements were made spectrophotometrically at 25 °C and different pH values (pH 6.2–8.5), employing a GBC 916 UV/Vis spectrophotometer with a thermostatic cell compartment. Reactions were initiated by injecting 30 μl of a 0.005 mol dm^{-3} stock solution of PNPP into 3 ml of buffer solution containing the desired reagents. Kinetic data were obtained by observing the rate of appearance of *p*-nitrophenol at 400 nm. The apparent first-order rate constants were obtained on fitting an equation ($\ln(A_t - A_\infty) - \ln(A_0 - A_\infty) = -k_{obsd}t$) by a non-linear least-squares treatment, and its average relative standard deviation is smaller than 1.5%.

3. Results and discussion

3.1. Apparent rate constants for hydrolysis of PNPP at pH 7.00 and 25 °C

The ligands **1**–**3** are all soluble, so the kinetics study was carried out in buffer and in buffered micellar solutions. The apparent rate constants (k_{obsd}) of the reaction shown in Table 1 were obtained by monitoring the liberation of *p*-nitrophenol from the substrate under the conditions of excess metal ion and ligand over the substrate at pH 7.00 and 25 °C.

Table 1 indicates that the uncatalyzed rate constant in buffer is $k_0 = 1.32 \times 10^{-5}$ s^{-1} at pH 7.00 and 25 °C. The surfactants CTAB and Brij35 showed little rate enhancement effect on hydrolysis of PNPP. Little rate enhancement was observed when the ligands **1**–**3** catalyzed the hydrolytic reaction in buffer solution or in micellar solution. However, remarkable rate acceleration was observed when complexes formed from these ligands with Cu^{2+} catalyzed the hydrolytic reaction. The apparent rate constants (k_{obsd}) followed the order: ligand **2** > **3** > **1**, which may be attributed to the different structure of the ligands and the different microenvironments of the micelles.

Table 1
Apparent rate constants ($k_{obsd} \times 10^3/s^{-1}$) for the hydrolysis of PNPP in metallomicellar system at pH 7.00 and 25 °C[a]

System		Cu^{2+}
–	0.0132	2.730
1	0.0226	27.600
2	0.0595	57.570
3	0.0457	30.490
CTAB	0.0213	24.420
1 + CTAB	0.0134	58.390
2 + CTAB	0.0462	97.040
3 + CTAB	0.0142	84.830
Brij35	0.0239	5.310
1 + Brij35	0.0337	20.840
2 + Brij35	0.0513	49.540
3 + Brij35	0.0402	37.100

[a] In 0.01 mol dm^{-3} Tris–TrisH$^+$ buffer [μ = 0.1 (KNO_3)]. [CATB] = 0.01 mol dm^{-3}, [Brij35] = 0.001 mol dm^{-3}, [PNPP] = 5×10^{-5} mol dm^{-3}, [ligand] = [Cu] = 1×10^{-3} mol dm^{-3}.

3.2. Stoichiometry of metal complexes in reaction systems

A convenient method for determining the chelating stoichiometry of metal complexes is the kinetic version of Job plots shown in Figs. 1 and 2, in which the apparent rate constants (k_{obsd}) are plotted as a function of the mole fraction (r) of a ligand or metal ion, keeping their total concentration constant [22,24,25]. Fig. 1 indicates that for three ligands, r values corresponding to the maximum k_{obsd} are all at about 0.35, suggesting that the 2:1 complexes (metal:ligand) are the active species in CTAB micellar solutions. From Fig. 2, the rate maximums of three plots are all attained at about $r = 0.67$, indicating that the 1:2 complexes (metal:ligand) are the active species in Brij35 micellar solution.

3.3. The ternary complex kinetic model for metallomicellar catalysis

Generally, the rates of the hydrolysis of PNPP in a metallomicelle are dependent on both metal ion and ligand concentrations. In the metallomicellar system, equilibrium exists between ligand (L), metal ion (M), and substrate (S). On the basis of the phase-separation model of micelle [23], metallomicelle-catalyzed reaction can be supposed to take place in the bulk phase and the metallomicellar phase simultaneously to afford the products (P):

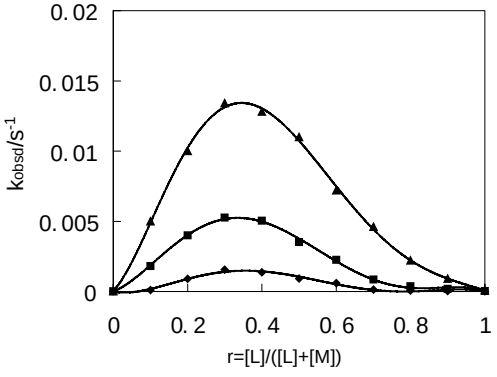

Fig. 1. Job plots for the ligands **1** (◆), **2** (■), and **3** (▲), and Cu^{2+} ion complexations as measured by the rates of hydrolysis of PNPP at 25 °C, pH 7.00 in 0.01 mol dm^{-3} CTAB; [L] + [Cu^{2+}] = 1×10^{-3} mol dm^{-3} and [PNPP] = 5×10^{-5} mol dm^{-3}.

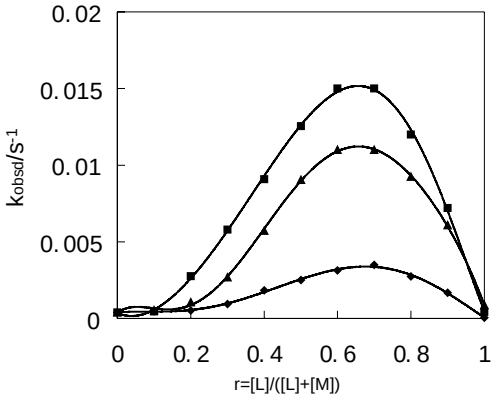

Fig. 2. Job plots for the ligands **1** (◆), **2** (■), and **3** (▲), and Cu^{2+} ion complexations as measured by the rates of hydrolysis of PNPP at 25 °C, pH 7.00 in 0.001 mol dm^{-3} Brij35; [L] + [Cu^{2+}] = 1×10^{-3} mol dm^{-3} and [PNPP] = 5×10^{-5} mol dm^{-3}.

$$\begin{cases} n\mathrm{L} + m\mathrm{M} \overset{K_\mathrm{M}}{\rightleftharpoons} \mathrm{M}_m\mathrm{L}_n \\ \mathrm{M}_m\mathrm{L}_n + \mathrm{S} \overset{K_\mathrm{T}}{\rightleftharpoons} \mathrm{M}_m\mathrm{L}_n\mathrm{S} \\ \mathrm{M}_m\mathrm{L}_n\mathrm{S} \overset{k'_\mathrm{N}}{\rightarrow} \mathrm{P} \\ \mathrm{S} \overset{k'_0}{\rightarrow} \mathrm{P} \end{cases} \quad (1)$$

$$K_\mathrm{M} = \frac{[\mathrm{M}_m\mathrm{L}_n]}{[\mathrm{M}]^m[\mathrm{L}]^n} \quad (2)$$

$$K_\mathrm{T} = \frac{[\mathrm{M}_m\mathrm{L}_n\mathrm{S}]}{[\mathrm{M}_m\mathrm{L}_n][\mathrm{S}]} \quad (3)$$

$$k'_0 = k_0 + k_\mathrm{M}[\mathrm{M}] + k_\mathrm{L}[\mathrm{L}] \quad (4)$$

where K_M is the association constant between m metal ions and n ligands, K_T the association constant between a binary complex ($\mathrm{M}_m\mathrm{L}_n$) and a substrate, k'_N and k'_0 the apparent first-order rate constants for product formation in the metallomicellar phase and in the bulk phase, respectively; k_0 the first-order rate constant due to the buffer; k_L and k_M the second-order rate constants due to the ligand and metal ion alone; [L], [M], and [S] the concentrations of ligand, metal ion, and substrate in the bulk phase, respectively; [$\mathrm{M}_m\mathrm{L}_n$] the concentration of m metal ions or n ligands in the metallomicellar phase, and [$\mathrm{M}_m\mathrm{L}_n\mathrm{S}$] the concentration of substrate in the metallomicellar phase.

$$[\mathrm{S}] = [\mathrm{S}]_\mathrm{T} - [\mathrm{M}_m\mathrm{L}_n\mathrm{S}] \quad (5)$$

$$[\mathrm{M}] = [\mathrm{M}]_\mathrm{T} - m[\mathrm{M}_m\mathrm{L}_n] \quad (6)$$

$$[\mathrm{L}] = [\mathrm{L}]_\mathrm{T} - n[\mathrm{M}_m\mathrm{L}_n] \quad (7)$$

where $[L]_T$, $[M]_T$, and $[S]_T$ are the total concentrations of ligand, metal ion and substrate, respectively.

Substituting Eqs. (6) and (7) for Eq. (2) and neglecting the high-order terms of $[M_mL_n]$, we have

$$[M_mL_n] = \frac{K_M[M]_T^m[L]_T^n}{1 + n^2K_M[M]_T^m[L]_T^{n-1} + m^2K_M[L]_T^n[M]_T^{m-1}} \quad (8)$$

According to the rate law, rate equation of reaction (1) can be written as

$$r = k_{obsd}[S]_T = k'_N[M_mL_nS] + k'_0[S] \quad (9)$$

Combination of Eqs. (5) and (9) and rearrangement give

$$k_{obsd} = \frac{k'_0 + (k'_N[M_mL_nS]/[S])}{1 + ([M_mL_nS]/[S])} \quad (10)$$

Substituting Eq. (3) for Eq. (10) and rearranging give

$$\frac{1}{k_{obsd} - k'_0} = \frac{1}{K_T(k'_N - k'_0)[M_mL_n]} + \frac{1}{k'_N - k'_0} \quad (11)$$

Eq. (11) is the ternary complex kinetic equation for metallomicellar catalysis. The ternary complex kinetic equation for metallomicellar inhibition can be written as

$$\frac{1}{k'_0 - k_{obsd}} = \frac{1}{K_T(k'_0 - k'_N)[M_mL_n]} + \frac{1}{k'_0 - k'_N} \quad (12)$$

Substituting Eq. (8) for Eq. (11) and rearranging give rise to

$$\frac{1}{k_{obsd} - k'_0} = \frac{1}{K_T(k'_N - k'_0)K_M[M]_T^m[L]_T^n} + \frac{n^2}{K_T(k'_N - k'_0)[L]_T} + \frac{m^2}{K_T(k'_N - k'_0)[M]_T} + \frac{1}{k'_N - k'_0} \quad (13)$$

Substituting Eq. (8) for Eq. (12) and rearranging give rise to

$$\frac{1}{k'_0 - k_{obsd}} = \frac{1}{K_T(k'_0 - k'_N)K_M[M]_T^m[L]_T^n} + \frac{n^2}{K_T(k'_0 - k'_N)[L]_T} + \frac{m^2}{K_T(k'_0 - k'_N)[M]_T} + \frac{1}{k'_0 - k'_N} \quad (14)$$

To obtain the values of $k_{N'}$, K_M, and K_T, the consecutive graphic method should be used. When $m = 2$, $n = 1$ in the CTAB micelle solution, from Eq. (13), the plots of $1/(k_{obsd} - k'_0)$ versus $1/[L]_T$ should give straight lines. The intercept, I, and slope, Q, of the straight line are, respectively, expressed as

$$I = \frac{1}{k'_N - k'_0} + \frac{4}{K_T(k'_N - k'_0)[M]_T} \quad (15)$$

$$Q = \frac{1}{(k'_N - k'_0)K_T} + \frac{1}{K_TK_M(k'_N - k'_0)[M]_T^2} \quad (16)$$

According to Eqs. (15) and (16), the plots of I versus $1/[M]_T$ and Q versus $1/[M]_T^2$ would allow estimations of $k_{N'}$, K_M, and K_T. When $m = 2$, $n = 1$ in the CTAB micelle solution, from Eq. (14), the plots of $1/(k'_0 - k_{obsd})$ versus $1/[L]_T$ should give straight lines. The intercept, I, and slope, Q, of the straight line are, respectively, expressed as

$$I = \frac{1}{k'_0 - k'_N} + \frac{4}{K_T(k'_0 - k'_N)[M]_T} \quad (17)$$

$$Q = \frac{1}{(k'_0 - k'_N)K_T} + \frac{1}{K_TK_M(k'_0 - k'_N)[M]_T^2} \quad (18)$$

According to Eqs. (17) and (18), the plots of I versus $1/[M]_T$ and Q versus $1/[M]_T^2$ would allow estimations of k'_N, K_M, and K_T.

When $m = 1$, $n = 2$ in the Brij35 micelle solution, from Eq. (13), the plots of $1/(k_{obsd} - k'_0)$ versus $1/[M]_T$ should give straight lines. The intercept, I, and slope, Q, of the straight line are, respectively, expressed as

$$I = \frac{1}{k'_N - k'_0} + \frac{4}{K_T(k'_N - k'_0)[L]_T} \quad (19)$$

$$Q = \frac{1}{(k'_N - k'_0)K_T} + \frac{1}{K_TK_M(k'_N - k'_0)[L]_T^2} \quad (20)$$

According to Eqs. (19) and (20), the plots of I versus $1/[L]_T$ and Q versus $1/[L]_T^2$ would also allow estimations of k'_N, K_M, and K_T.

3.4. Discussion

The hydrolysis of PNPP was investigated at room temperature and in near neutral solutions because the nature enzymes show their extraordinary catalytic activities under very mild conditions. In the high pH region (pH > 8.50), no first-order rate constants were obtained since precipitation occurred.

Table 1 shows complexes formed by metal ion Cu^{2+} and these ligands in the micellar solutions markedly enhanced the rate of the hydrolysis. In micellar solution of cationic surfactant CTAB, the catalytic effect on hydrolysis of PNPP was larger than that in micellar solution of non-ionic surfactant Brij35 and this may be ascribed to the hydrophobicity and the electrostatic interaction of the surfactant CTAB. One of the most important processes leading to micellar effects on reactions is the solubilization of reactants in micellar interiors [15]. In reaction systems studied in this paper, the substrate and the complex formed by metal ion (Cu^{2+}) and the ligands could be partially solubilized into micellar stern layer, where most reactions were considered to occur, and this could lead to the increase in local concentration of the reactants and then affect the reaction rate of the hydrolysis of PNPP when compared with the spontaneous hydrolytic rate of PNPP in buffer. From Table 1, it could also be seen that, in the absence of metal ion, the hydrolytic rate constant for PNPP catalyzed by three ligands in buffered solution

were roughly the same as that in non-ionic micellar solution, which may be attributed to the structure of the Brij35 micelle. As non-ionic surfactant, the Brij35 micellar surface mainly formed by twined long polyoxyethylene chains, which resulted in weak solubilization of water-soluble ligands and the substrate and then showed almost no effect on the hydrolytic reaction. In contrast, compared with the hydrolytic reaction of PNPP catalyzed by three ligands and metal ion (Cu^{2+}) in buffered solution, the rate constants were notably enhanced in cationic micellar solution. Although both CTAB and Brij35 micelles could provide the hydrophobic microenvironment for reactants, the catalytic effect on the hydrolysis of PNPP was widely different, and therefore the electrostatic interaction between the surfactants and the reactants most probably played an important role in CTAB micellar solution. In the hydrolytic process, cationic micelle could bring the substrate and the complexes into its Stern layer through electrostatic effect, which made the reaction occur easily. In addition, the positive head groups of CTAB and metal ion (Cu^{2+}) both could neutralize the negative charge developed from the intermediate, so the hydrolytic reaction of PNPP was clearly accelerated in CTAB micellar solution.

At the same time, during the hydrolytic processes, the reactants transferred between the water phase and the micellar phase in the hydrolysis of PNPP. For non-ionic surfactant Brij35 system, transfer of the reactants between water phase and micellar phase were mainly caused by thermal motion and hydrophobicity. However, besides thermal motion and hydrophobicity, the electrostatic interaction in cationic surfactant CTAB system was also involved in reactants transfer due to the fact that cationic CTAB micelle could either attract the reactive ions or repel them depending upon hydrophobicity and their electrical charge, and this effect was also favorable for the hydrolysis of PNPP. Therefore, the micelle of cationic surfactant was advantageous in the hydrolysis of PNPP.

From Figs. 3 and 4, it is shown that apparent rate constant of hydrolysis of PNPP decreased with increasing ligand or metal ion concentration in complex **1**, whereas for complexes **2** and **3**, apparent rate constant increased with increasing ligand or metal ion concentration, and this phenomenon may be contributed to the different structure and the different hydrophobicity of these ligands. In contrast with the bridged structure of the ligand **2** containing a 10-carbon atom alkyl and the ligand **3** containing a benzene, the ligand **1** contains a three-carbon atom alkyl bridge; thus, the hydrophobicity of three ligand bridges follows the order: ligand **2** > **3** > **1**. From Table 1, it is shown that, in the absence of metal ion, apparent rate constant for PNPP catalyzed by three ligands follows the order: ligand **2** > **3** > **1**, either in buffered solution or in micellar solution. From the relationship between the hydrophobicity and the solubility, it could follow that the stronger the ligand's hydrophobicity is, the easier it dissolves in the micelles of surfactants and therefore the larger the apparent rate constant is. That is to say, ligand **1** with three-carbon atom alkyl bridge is most soluble in water among three ligands, and thus, this ligand exists mainly in bulk phase but not in micellar pseudo-phase, while the substrate (PNPP) may be partitioned between the bulk solvent and the micellar phase, which resulted in the separation of the reactants; therefore, the hydrolysis of PNPP in CTAB micellar solution is not enhanced by ligand **1**. From Table 2 and Fig. 5, it could be seen that, in CTAB micellar solution, the activity of different ligands complexing with the metal ion Cu^{2+} followed the order: **3** > **2** > **1**. That is to say, the hydrolytic rate constant of PNPP for complex **1** was smaller than that of complexes **2** and **3**. However, in Brij35 micellar solution, the results showed that the activity

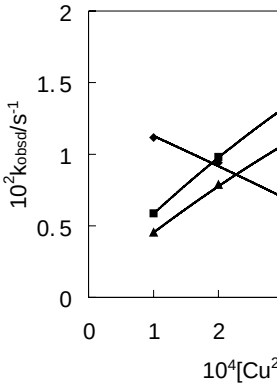

Fig. 3. Pseudo-first-order rate constants for the hydrolysis of PNPP in 0.01 mol dm^{-3} CTAB at 25 °C, pH 7.00 as the function of Cu^{2+} concentration; ligands **1** (◆), **2** (■), and **3** (▲). [L] = 1×10^{-4} mol dm^{-3} and [PNPP] = 5×10^{-5} mol dm^{-3}.

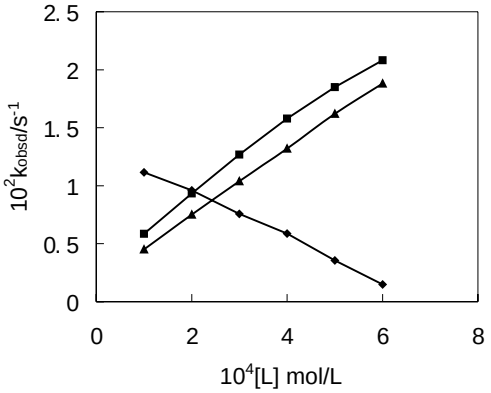

Fig. 4. Pseudo-first-order rate constants for the hydrolysis of PNPP in 0.01 mol dm^{-3} CTAB at 25 °C, pH 7.00 as the function of ligand concentrations; ligands **1** (◆), **2** (■), and **3** (▲). [Cu^{2+}] = 1×10^{-4} mol dm^{-3} and [PNPP] = 5×10^{-5} mol dm^{-3}.

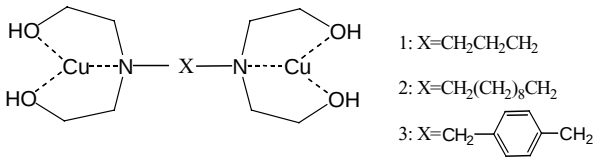

Fig. 5. The structure of complex in CTAB micellar solution.

Table 2
pH dependencies of k'_N, K_M, and K_T at 25 °C for Cu^{2+} complexes in metallomicellar system

pH	L	CTAB			Brij35		
		$k'_N \times 10^2$ (s^{-1})	$K_M \times 10^{-7}$ (mol dm^{-3})	$K_T \times 10^{-4}$ (mol dm^{-3})	$k'_N \times 10^2$ (s^{-1})	$K_M \times 10^{-7}$ (mol dm^{-3})	$K_T \times 10^{-4}$ (mol dm^{-3})
7.00	**1**	0.23	64.40	2.34	5.14	2.23	2.43
	2	2.83	18.00	12.80	8.86	1.95	3.38
	3	4.38	15.80	99.50	3.94	3.13	1.58

in different ligand complexing with Cu^{2+} followed the order: **2** > **1** > **3** and this may be due to the different active species of 2:1 ratio of metal:ligand in CTAB micellar solution, the inhibition of complex **1** on hydrolysis of PNPP, and 1:2 ratio of metal:ligand in Brij35 micellar solution. As illustrated in Fig. 6, the stronger the rigidity of the bridge of the ligand, the farther the distance between the hydroxyl group generating the nucleophile and the substrate coordinated to metal ion, which is unfavorable for the catalytic hydrolysis of the substrate. In other words, the stronger the rigidity of the bridge of the ligand, the lower the activity in the complex promoted hydrolysis of PNPP. In contrast, the flexible bridge of the ligand makes the hydroxyl group approach the substrate coordinated to metal ion to cause the fast catalytic hydrolysis of PNPP.

From Table 2, in addition, it could be also seen that the binding constants (K_M and K_T) were closely related to the hydrolytic rates. In CTAB and Brij35 micellar solutions, for the three ligands, the sequence of the binding constants (K_M) of binary complexes (M_mL_n) was opposite to that of the binding constants (K_T) of ternary complexes and the catalytic rate constants (k'_N). This is easy to understand that the larger the binding constant of the binary complexes, the stronger the association of Cu^{2+} and the ligand. In other words, if K_M is larger, the binary complex is more stable, and then the binary complex associates the substrate less strongly, so the value of K_T would be smaller than that of complexes with lower K_M, and this resulted in the weaker catalytic hydrolysis and smaller value of hydrolytic rate (k'_N).

3.5. pH-rate profile

From the results obtained, it was obviously shown that k'_N is pH-dependent, in other words, k'_N is related to the acid dissociation constant (K_a) of the hydroxyl group of the ternary complex in the reaction system

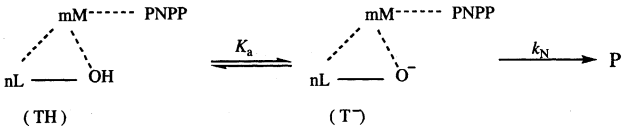

(21)

where TH is the undissociated complex, T^- the dissociated complex anion assumed to be the active species in metallomicellar phase and k_N the first-order rate constant which is pH-independent.

Then, we have

$$[M_mL_nS] = [TH] + [T^-] \quad (22)$$

and

$$K_a = \frac{[T^-][H^+]}{[TH]} \quad (23)$$

By substituting Eq. (22) in Eq. (23), we obtain

$$[T^-] = \frac{K_a[M_mL_nS]}{[H^+] + K_a} \quad (24)$$

The rate equation in the metallomicellar phase can be expressed as

$$r' = k'_N[M_mL_nS] = k_N[T^-] \quad (25)$$

Substituting Eq. (24) in Eq. (25) and rearranging, we have

$$\frac{1}{k'_N} = \frac{1}{k_N} + \frac{1}{k_N K_a}[H^+] \quad (26)$$

On the basis of Eq. (26), the k_N and K_a values can be afforded from the slope and the intercept of the plot $1/k'_N$ versus $[H^+]$. The results are shown in Table 3 and Figs. 7 and 8.

According to the results in the present paper, the rate constants for hydrolysis of PNPP in the presence of ligand **1** are

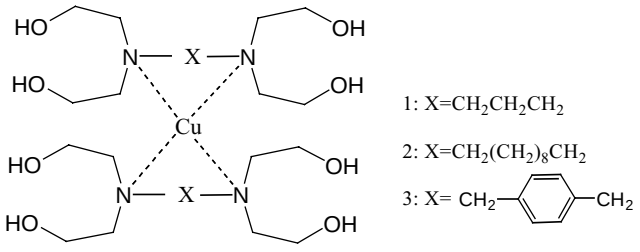

Fig. 6. The structure of complex in Brij35 micellar solution.

Table 3
k_N and pK_a of the hydrolysis of PNPP in the metallomicellar systems with Cu^{2+} and ethoxyl-diamine ligand

L	CTAB		Brij35	
	k_N (s^{-1})	pK_a	k_N (s^{-1})	pK_a
1	0.00563	7.12	0.211	7.48
2	0.185	7.71	0.379	7.49
3	0.551	8.05	0.177	7.80

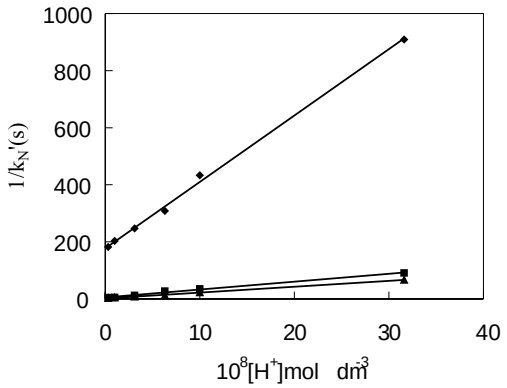

Fig. 7. pH-rate profile for release of *p*-nitrophenol from PNPP in the Cu^{2+} ion and CTAB micelle system at 25 °C; ligands **1** (◆), **2** (■), and **3** (▲).

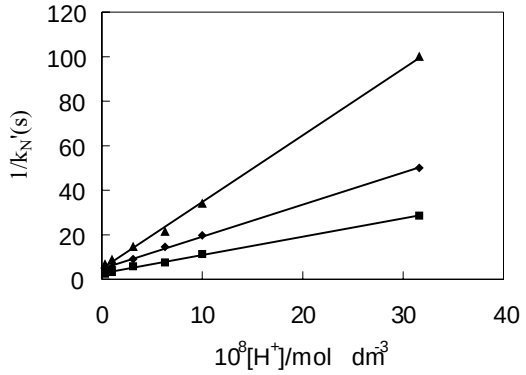

Fig. 8. pH-rate profile for release of *p*-nitrophenol from PNPP in the Cu^{2+} ion and Brij35 micelle system at 25 °C; ligands **1** (◆), **2** (■), and **3** (▲).

significantly small owing to the relatively low hydrophobicity of this ligand when compared with those of other two ligands. In addition, k'_N is pH-dependent. Due to the low hydrophobicity of ligand **1**, the rate constants for hydrolysis of PNPP catalyzed by complex formed by ligand **1** increased relatively little compared with that by other two ligands with the increasing pH value of CTAB micellar solution, and thus it is evident that the real first-order rate constants calculated from k_{obsd} in CTAB micellar system are also small. As a result, reciprocal of such small k'_N value for complex **1** would exhibit a large intercept as shown in Fig. 7.

From Figs. 7 and 8 and Table 3, it can be seen that the k_N values of the fully dissociated hydroxyl group of complexes of the copper ion are also related to the structure of the different ligands and follow the same sequence as that of corresponding k'_N values. Also, the real rate constant (k_N) in metallomicellar phase is several times larger than k'_N, not to mention k_0, especially for complex **3** in the CTAB micelle, where its real rate constant (k_N) is up to 0.551 s^{-1}, suggesting that the rate constant of hydrolysis of PNPP in CTAB metallomicelle is more than 4×10^4 times larger than that in buffer solution. This indicates that the metallomicellar system investigated in this paper, to a certain extent, mimics the reaction of enzymatic catalysis not only in terms of microenvironment but also in terms of active center.

4. Conclusion

It is necessary for us to establish different kinetic models for different reaction systems in micellar solutions to understand the mechanism of artificial enzymatic catalyst more clearly. The kinetic model proposed in this paper is applicable to the cases in which metallomicelle formed by complexes of different chelating ratios catalyzed the hydrolysis of PNPP.

Here some interesting results should be noticed:

(1) The chelating ratios of the ligand to Cu^{2+} are not the same in different micellar solutions due to the microenvironment: in CTAB micellar solution, the complexes with the ratios of 2:1 (metal:ligand) were obtained; in contrast, the complexes with the ratios of 1:2 (metal:ligand) were the active species in Brij35 micelle.
(2) The apparent first-order rate constants (k'_N) of the hydrolysis of PNPP depend on the structure of the bridged ligands investigated and the microenvironment of reaction. In CTAB micelle, the more hydrophobic the ligand, the larger the k'_N; whereas in Brij35 micelle, the stronger flexibility the ligand has, the larger the k'_N. This case is also true of real rate constants (k_N). In the systems studied in this paper, k_N values are much larger than the apparent first-order rate constants (k_0) for the product formation in the buffer solution, in particular, when complex **3** in the CTAB micelle catalyzed the hydrolysis of PNPP, its k_N is larger than k_0 up to 4×10^4 times.
(3) In complex **1** catalyzing the hydrolysis of PNPP, apparent rate constant decreased with increasing ligand or metal ion concentration. However, for complexes **2** and **3** catalyzing the hydrolysis of PNPP, apparent rate constant increased with increasing ligand or metal ion concentration and this phenomenon may be due to the structure and the hydrophobicity of the ligands.

Acknowledgements

This work was supported by the National Natural Science Foundation of China (Grants: 29873031, 20173038, 20132020).

References

[1] T. Eiki, M. Mori, S. Kawada, K. Matsushima, W. Tagaki, Chem. Lett. (1980) 1431.
[2] J. Chin, Acc. Chem. Res. 24 (1991) 145.
[3] S.Q. Cheng, X.Q. Yu, X.C. Zeng, J. Dis. Sci. Tech. 20 (1999) 1821.
[4] R. Fornasier, P. Scrimin, P. Tecilla, U. Tonellato, J. Am. Chem. Soc. 111 (1989) 224.

[5] P. Scrimin, P. Tecilla, U. Tonellato, J. Org. Chem. 56 (1991) 161.
[6] D.W. Christianson, W.N. Lipscomb, Acc. Chem. Res. 22 (1989) 62.
[7] J.E. Coleman, J.F. Chlebowski (Eds.), Advanced Inorganic Biochemistry, Elsevier, New York, 1979.
[8] F. Tafesse, S.S. Massoud, R.M. Milburn, Inorg. Chem. 24 (1985) 2591.
[9] J. Chin, X. Zou, Can. J. Chem. 65 (1987) 1882.
[10] J.R. Morrow, W.C. Trogler, Inorg. Chem. 27 (1988) 3387.
[11] T.H. Fife, M.P. Pujari, J. Am. Chem. Soc. 112 (1990) 5551.
[12] M.A.D. Rosch, W.C. Trogler, Inorg. Chem. 29 (1990) 2409.
[13] T.H. Fife, M.P. Pujari, J. Am. Chem. Soc. 110 (1988) 7790.
[14] R.W. Hay, N. Govan, J. Chem. Soc., Chem. Commun. (1990) 714.
[15] S. Tascioglu, Tetrahedron 52 (1996) 11113.
[16] S.Q. Cheng, X.C. Zeng, X.G. Meng, X.Q. Yu, J. Colloid Interf. Sci. 224 (2000) 333.
[17] Y. Xiang, X.C. Zeng, S.Q. Cheng, Y.T. Li, J.Q. Xie, J. Colloid Interf. Sci. 235 (2001) 114.
[18] X.C. Zeng, S.Q. Cheng, X.Q. Yu, Z. Huang, J. Dis. Sci. Tech. 20 (1999) 1581.
[19] S.Q. Cheng, X.C. Zeng, J. Dis. Sci. Tech. 21 (2000) 655.
[20] Y. Xiang, X.C. Zeng, S.Q. Cheng, Y.T. Li, J.Q. Xie, J. Dis. Sci. Tech. 21 (2000) 857.
[21] D.S. Sigman, C.T. Jorgensen, J. Am. Chem. Soc. 94 (1972) 1724.
[22] T. Fujita, Y. Inaba, K. Ogino, W. Tagaki, Bull. Chem. Soc. Jpn. 61 (1988) 1661.
[23] F.M. Menger, C.E. Portnoy, J. Am. Chem. Soc. 89 (1967) 4698.
[24] F. Mancin, P. Tecilla, U. Tonellato, Langmuir 16 (2000) 227.
[25] S. Bhattacharya, K. Snehalatha, V.P. Kumar, J. Org. Chem. 68 (2003) 2741.